Resolving the relationship between capacity/voltage decay and phase transition by accelerating the layered to spinel transition.

Qi Pang,[a] Mengke Zhang,[a] Yang Song,[a] Yueying Liu,[a] Manqi Tang,[a] Lang Qiu*[a], Yao Xiao*[b, c], Xiaodong Guo*[a]

a School of Chemical Engineering, Sichuan University, Chengdu 610065, P.R. China.

b College of Chemistry and Materials Engineering, Wenzhou University, Wenzhou 325035, P.R.

c Key Laboratory of Advanced Energy Materials Chemistry (Ministry of Education), Nankai University, Tianjin 300071, China

*Corresponding authors

Lang Qiu - School of Chemical Engineering, Sichuan University, Chengdu 610065, P.R. China; E-mail: qiulang2023@scu.edu.cn

Yao Xiao - College of Chemistry and Materials Engineering, Wenzhou University, Wenzhou 325035, P.R. China; E-mail: xiaoyao@wzu.edu.cn

Xiaodong Guo - School of Chemical Engineering, Sichuan University, Chengdu 610065, P.R. China; E-mail: xiaodong2009@163.com

Experimental Section

1.1 Materials Preparation

The $Ni_{0.25}Mn_{0.75}(OH)_2$ precursor for the preparation of obtained via the co-precipitation method has been reported in the literature. Mixing the as-obtained precursor with $LiOH{\cdot}H_2O$ (Li: TM ratio = 1.07:1) and then. The mixture was further ground for 30 min, heated at 500 °C for 6 h and 970 °C for 12 h at a ramp rate of 5 °C min^{-1}, and then cooled to room temperature naturally to yield the pristine materials.

A certain proportion of Fe $(NO_3)_3$-$9H_2O$ and NH_4F was dissolved in anhydrous ethanol and stirred until the solution changed from light yellow to a clear, clarified liquid. (The FeF_3 content in the sample solution was 3 wt%, respectively.) The prepared LRM powder was then homogeneously dispersed in ethanol to obtain solution A. The solution A was placed in an oil bath at 70°C. The solution was stirred until the solvent was completely evaporated. Stirring was done until the solvent was completely evaporated. Then, the obtained powder was dried in an oven at 100°C for 12 hours. Finally, the dried powder was calcined at 400°C under argon atmosphere for 4 hours to obtain LFF3.

1.2 Materials characterization

The crystal structure of Li-rich materials was characterized by using powder X-ray diffraction (XRD) with a Cu Kα radiation of Bruker D8 Advance in the 2Θ range of 10°-80°. And FULLPROF software was

applied for Rietveld refinement. Raman spectra was collected by Renishaw in Via equipment, with a laser of 532 nm. The morphology of the material was observed by scanning electron microscopy (SEM, ZEISS Gemini SEM 300). Focused ion beam technique (FIB, FEI Strata 400S) was applied to the high-resolution transmission electron microscopy (HR-TEM) specimen preparation. The HR-TEM and selected area electron diffraction (SAED) images were conducted on FEI Talos-F200S. The working voltage for HR-TEM was 200 kV.

1.3 Electrodes fabrication

The composite electrodes were fabricated by using LRM and LFF3 as active materials (80 wt%), poly (vinylidene fluoride) as the binder (10 wt%), and acetylene black (10 wt%) as a conductive agent. The homogenous slurry was applied to an aluminum sheet and dried overnight in a vacuum at 100 °C to eliminate residual solvent. After drying, the electrodes were punched into 14×14 mm^2 squares (~2.5 mg cm^{-2}) and transferred into an Ar-filled glove box.

1.4 Electrochemical testing

CR2025 coin-type cells were assembled by using Li-mental as the negative electrode for half-cells and Celgard-2500 as the separator. The electrolyte was consisted of 1.0 M $LiPF_6$ with dissolved ethylene carbonate and dimethyl carbonate (volume ratio 1:1). The amount of electrolyte per cell during the assembling of cells was about 50 μl. The electrochemical

performance was tested using NEWWARE battery program in the voltage window of 2.0-4.8 V under 30 °C. The kinetic performance of the electrode was evaluated using constant current intermittent titration (GITT) technique, supplying a constant current of 0.1 C for 10 min and a subsequent relaxation for 60 min on an activated cell.

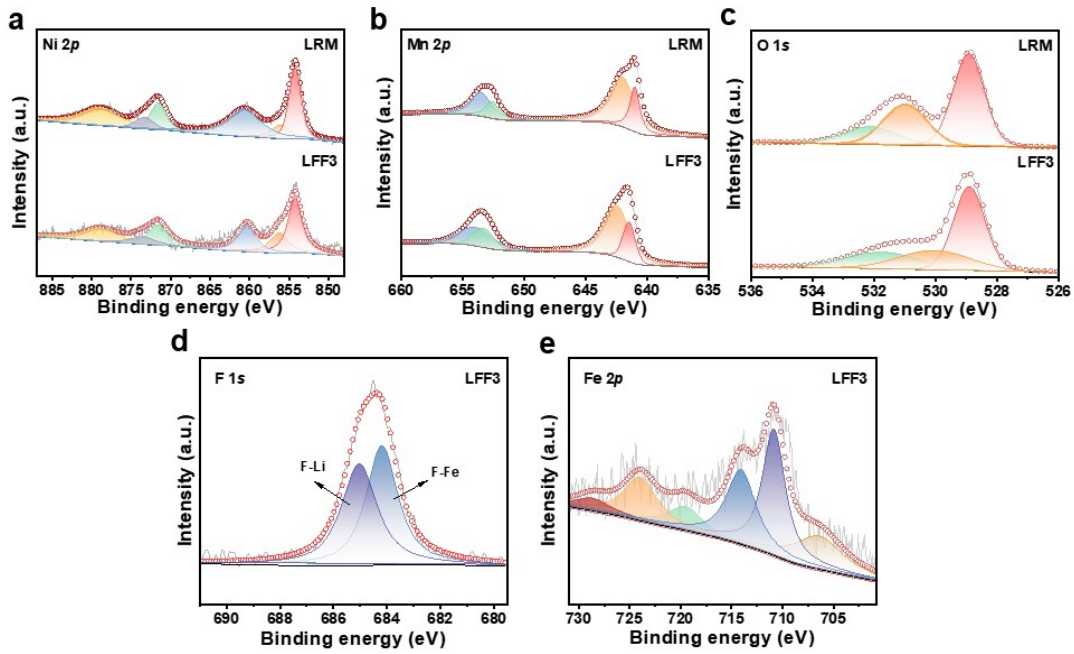

Fig. S1 The XPS spectra of (a) Ni 2*p*, (b) Mn 2*p*, (c) O 1*s* for LRM and LFF3, (d) F 1*s*, (e) Fe 2*p* for LFF3.

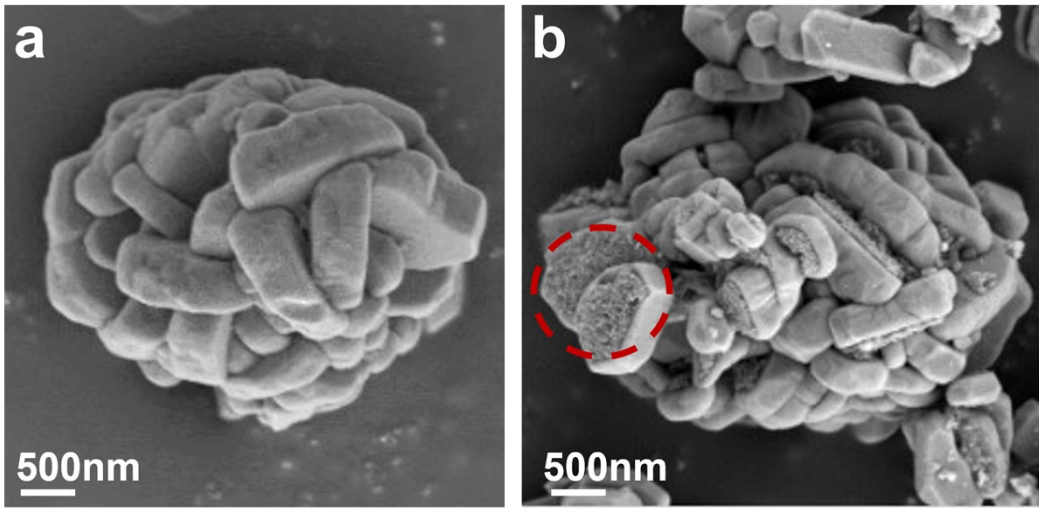

Fig. S2 SEM of LRM(a) and LFF3(b).

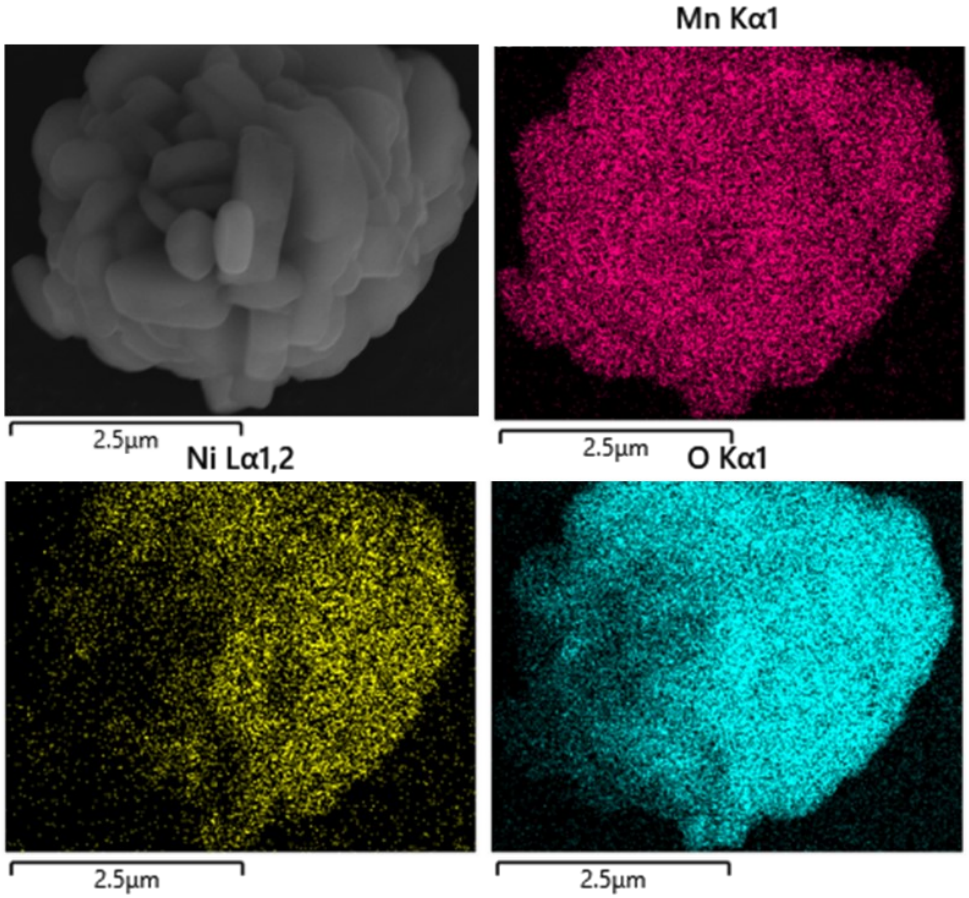

Fig. S3 The SEM mapping plots of LRM particles.

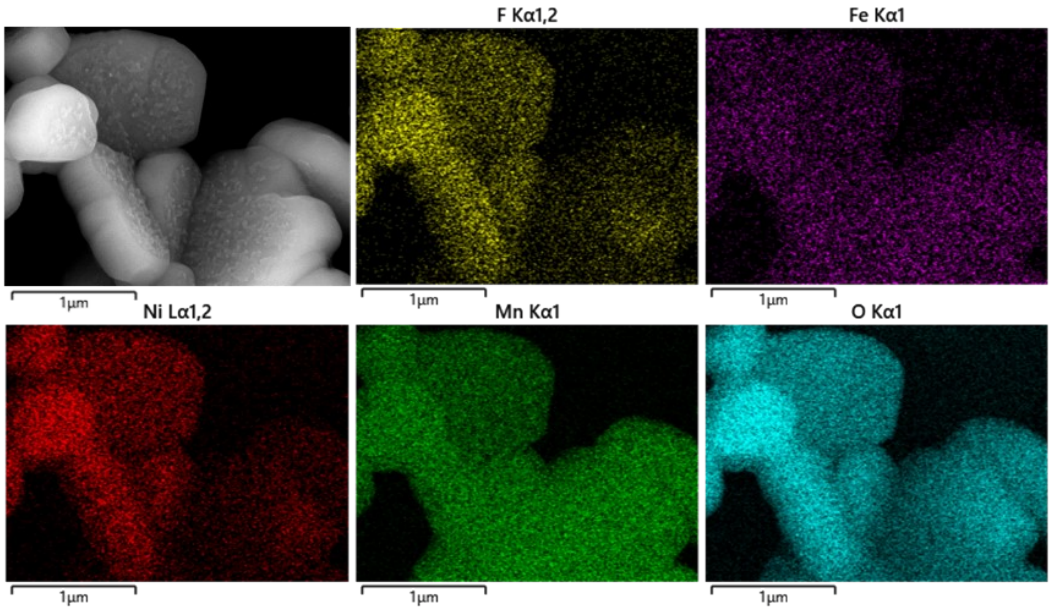

Fig. S4 The local SEM mapping plots of LFF3 particles.

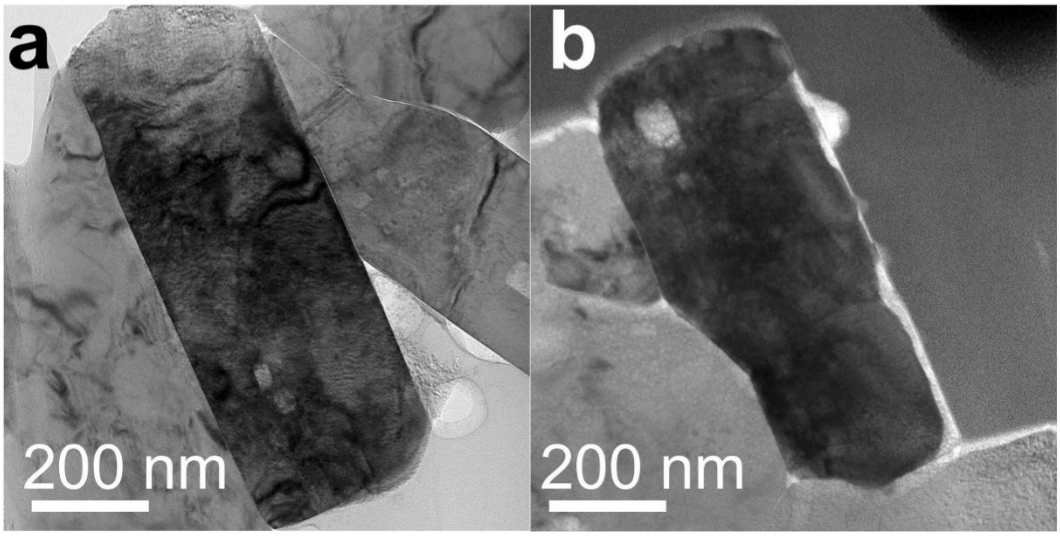

Fig. S5 The TEM of (a) LRM and (b) LFF3.

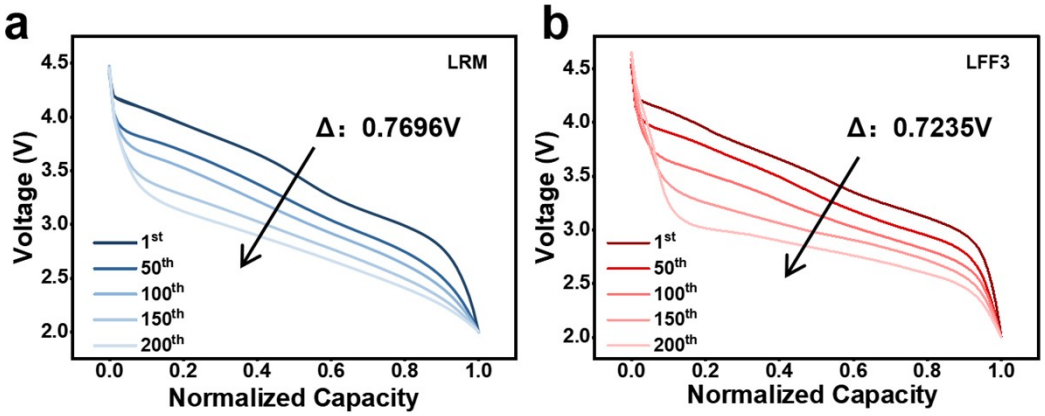

Fig. S6 Discharging curves of the (a) LRM and (b) LFF3 cycled at every 50 cycles in 200 cycles at 1 C.

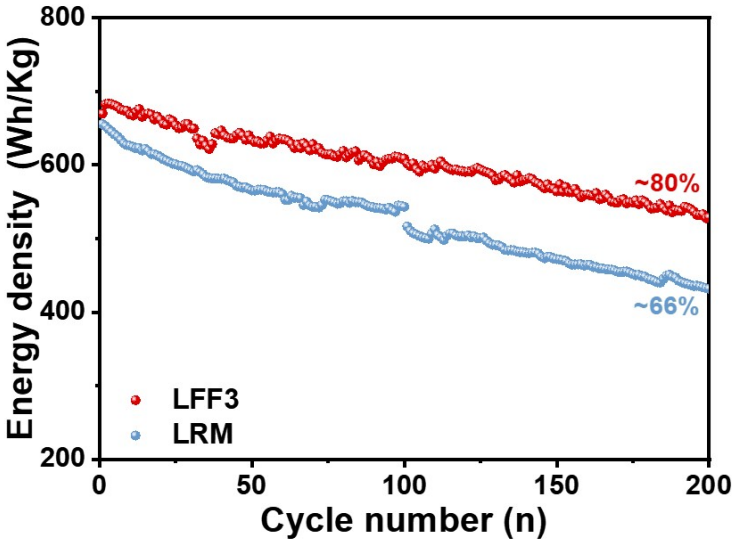

Fig. S7 Energy density of the LRM and LFF3 during 200 cycles.

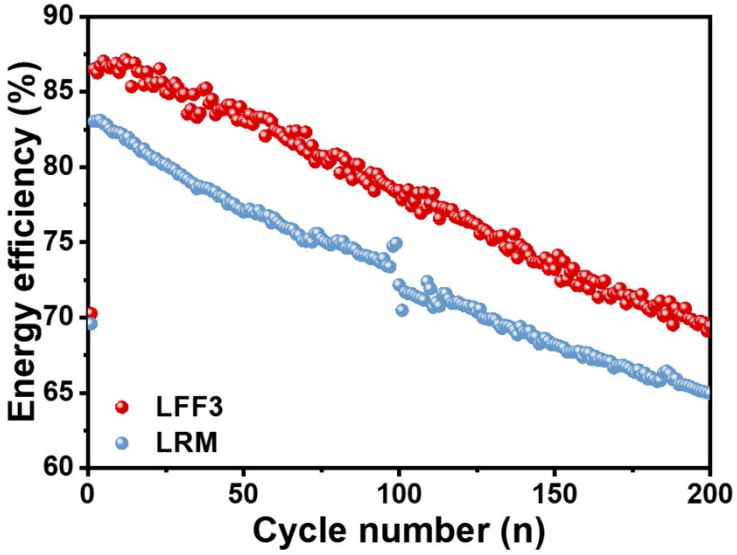

Fig. S8 Energy efficiency of the LRM and LFF3 during 200 cycles.

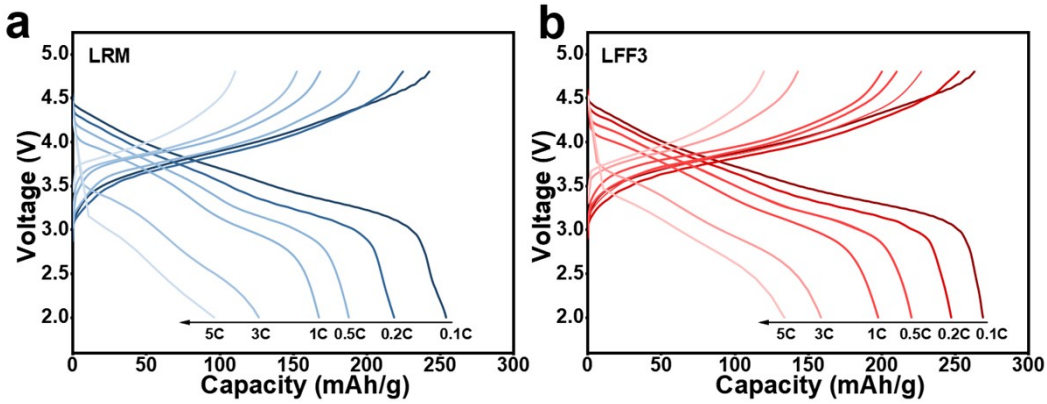

Fig. S9 Charge-discharge curves of the (a) LRM and (b) LFF3 at different rates.

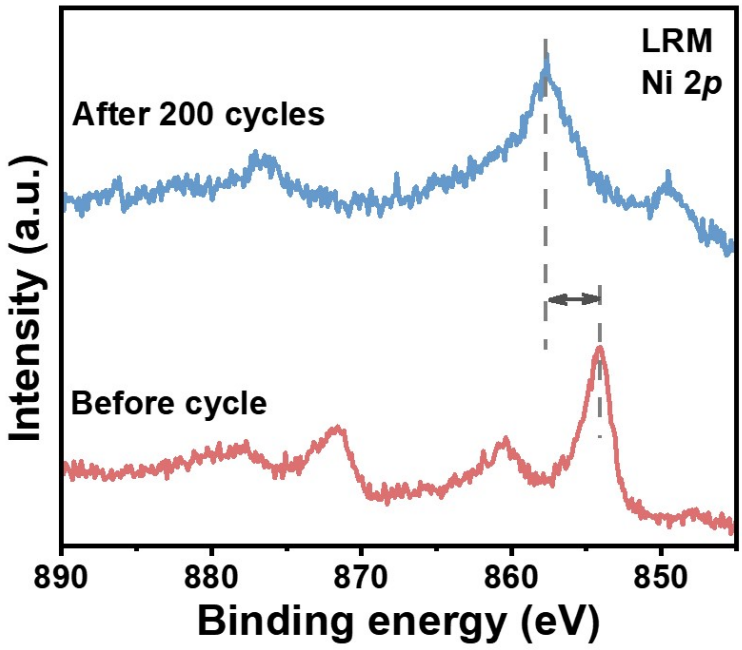

Fig. S10 The XPS spectra of Ni 2*p* for LRM.

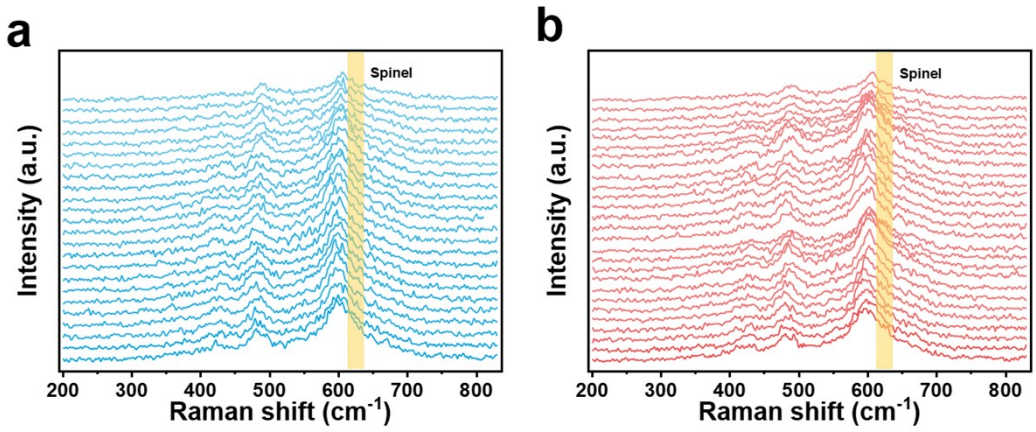

Fig. S11 Partial source data for Raman mapping of LRM (a) and LFF3 (b) after 200 cycles.

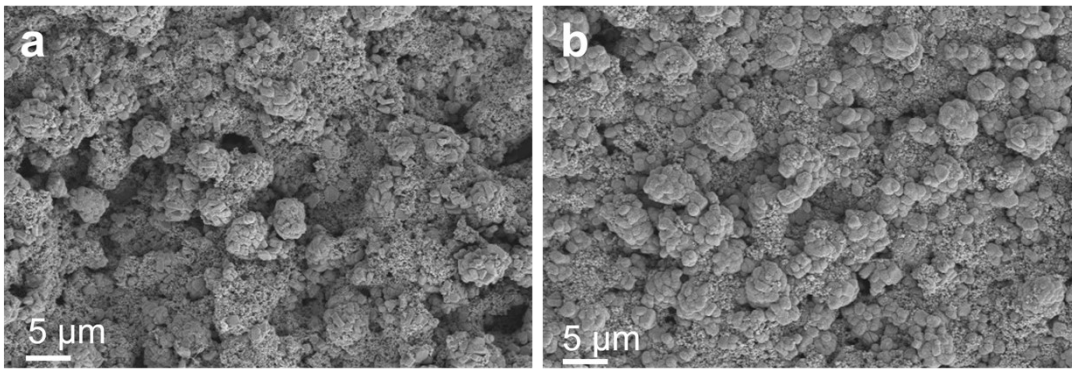

Fig. S12 SEM images of (a) LRM and (b) LFF3 after 200 cycles.

Table S1. The Rietveld refinement data for LRM and LFF3.

Sample	a[Å]	c[Å]	R_{WP} (%)	R_P (%)	Unit Cell Volume [Å^3]
LRM	2.8618(2)	14.2542(19)	1.53	1.1	101.10(1)
LFF3	2.8603(6)	14.2522(3)	1.45	1.08%	100.98(1)

Table S2. Lattice parameters and structural parameters of LRM after 200 cycles.

	Space group		
	$R\bar{3}m$	$Fd\bar{3}m$	$Fm\bar{3}m$
a[Å]	2.8860(4)	7.3449(1)	4.0684(9)
b[Å]	2.8860(4)	7.3449(1)	4.0684(9)
c[Å]	14.3348(1)	7.34491)	4.06849)
V[Å^3]	103.49(6)	393.60(2)	67.29(5)
Fraction(wt%)	95.92(8)	1.03(6)	3.04(6)
R_{wp}(%)		2.72	
R_p(%)		2.15	

Table S3. Lattice parameters and structural parameters of LFF3 after 200 cycles.

	Space group		
	$R\bar{3}m$	$Fd\bar{3}m$	$Fm\bar{3}m$
a[Å]	2.8854(4)	8.1316(1)	4.1745(4)
b[Å]	2.8854(4)	8.1316(1)	4.1745(4)
c[Å]	14.3236(9)	8.1316(1)	4.1745(4)
V[Å^3]	103.27(2)	537.69(6)	72.75(1)
Fraction(wt%)	88.32(7)	9.34(4)	2.33(7)
R_{wp}(%)		3.52	
R_p(%)		2.69	